

# Chapter 3

## Large Eddy Simulation of Atmospheric Boundary Layers

C.-H. Moeng

*National Center for Atmospheric Research, Boulder, USA.*

---

### Abstract

In this chapter, we describe the large-eddy simulation (LES) technique, review some important contributions that LES studies have made to planetary-boundary-layer (PBL) research, present the current status of PBL LES research, and discuss some future challenges for LES in simulating more complex PBL regimes.

---

### 1 Introduction

Turbulent motion in the planetary boundary layer (PBL) covers a wide range of scales. Largest turbulent eddies are confined to the PBL depth,  $z_i$ , and hence are on the order of several hundred meters to a couple of kilometers. (In nature, the PBL turbulent motion coexists with mesoscale motions, as shown in chapter 3, and thus it may sometimes be difficult to define the largest turbulent eddies from observations.) At the other end of the spectrum, the smallest turbulent eddies are at the Kolmogorov microscale,

$$\eta = (\nu^3/\epsilon)^{1/4}, \quad (1)$$

where  $\nu \sim 10^{-5}$  m<sup>2</sup>/s is the kinematic viscosity of air and  $\epsilon$  is the molecular dissipation rate. In equilibrium, the amount of energy dissipation should equal the amount of energy input from the energy-containing scale, so

$$\epsilon = u^3/\ell, \quad (2)$$

where  $u$  and  $\ell$  are the velocity and length scales of the energy-containing eddies. For a convective PBL,  $u \sim w_* \sim 1$  m/s, and  $\ell \sim z_i \sim 1$  km, hence  $\epsilon \sim 10^{-3}$  m<sup>2</sup>/s<sup>3</sup>.  $w_* \equiv ((g/T_0) z_i \overline{w\theta_0})^{1/3}$  is the convective velocity scale, where  $\overline{w\theta_0}$  is the surface heat flux. This gives  $\eta \sim 10^{-3}$  m. In other words, turbulent eddies in the PBL range from kilometers to millimeters in scale.

To numerically integrate the Navier-Stokes equations with adequate resolution for all these eddies requires at least  $10^{18}$  grid points. Of course we don't have (and will not have for some time) such computational power to perform this task. Fortunately, turbulence within the PBL has the following property: the largest eddies are responsible for most of the turbulent transport of heat, moisture, and momentum, which are the most important meteorological effects of PBL turbulence. Small eddies are mainly dissipative. This forms the basis for the large-eddy simulation (LES) technique, which explicitly calculates the important part of the turbulent motion and parameterizes the net effect of small eddies.

## 2 Overview of Large Eddy Simulation (LES)

### 2.1 The governing equations

The governing equations for LES are derived, as demonstrated in the following, from the Navier-Stokes equation, which is a set of basic dynamics equations of an incompressible fluid. The flow of fluid at any time,  $t$ , and space,  $x_i$ , is governed by

$$\frac{\partial u_i}{\partial t} + u_j \frac{\partial u_i}{\partial x_j} = X_i - \frac{1}{\rho} \frac{\partial p}{\partial x_i} + \nu \frac{\partial^2 u_i}{\partial x_j^2}, \quad (3)$$

where  $X_i$  is the  $i$ -component of the external force and  $p$  is pressure, and  $\rho$  is the air density. Expanding (3) over a hydrostatic equilibrium reference state and using the Boussinesq approximation, the external gravitational forcing in (3) can be written as  $\sim g_i \theta / T_0$ , where  $T_0$  is the temperature of the reference state.

Next, decompose the dependent variable, e.g.,  $u_i$ , into a volume-average,  $\tilde{u}_i$ , and the subgrid-scale fluctuating part within each volume,  $u_i''$ , i.e.,  $u_i = \tilde{u}_i + u_i''$ , (3) becomes

$$\frac{\partial \tilde{u}_i}{\partial t} + \tilde{u}_j \frac{\partial \tilde{u}_i}{\partial x_j} = + \frac{g_i}{T_0} \tilde{\theta} - \frac{1}{\rho_0} \frac{\partial \tilde{p}}{\partial x_i} - \frac{\partial \widetilde{u_i'' u_j''}}{\partial x_j}, \quad (4)$$

where the resolved-scale variable is defined as

$$\tilde{u}_i = \int \int \int_{\text{volume}} (u_i G) dx dy dz \quad (5)$$

using a spatial filter function  $G$  to filter out the small-scale turbulent motion (The molecular term associated with  $\nu$  is omitted in (4) because it is negligibly small for high- $R_e$  flows.) Turbulent motions are now split into two components: large (resolved-scale) eddies  $\tilde{u}_i$  and small (subgrid-scale, SGS) eddies  $u_i''$ , and (4) governs the LES flow field of  $\tilde{u}_i$ .

The net effect of SGS eddies, which are removed from the resolved flow field through the filtering procedure, shows up as the  $\partial u_i'' \tilde{u}_j'' / \partial x_j$  term in (4). SGS turbulent eddies are generated from nonlinear interaction (scrambling) of large eddies, thus do not depend sensitively on external flow conditions and are more isotropic in nature. The SGS effect is parameterized with a SGS model in LES. The most popular SGS model is based on the Smagorinsky-Lilly formula, where eddy viscosity depends on local wind shear and temperature gradient. This formula can be derived from the SGS turbulence kinetic energy (TKE) budget where the local shear and buoyancy productions are set to equal the molecular dissipation rate. Small turbulent eddies in the inertial subrange are known to have a  $-5/3$  energy spectrum. So if the LES grid mesh is in the inertial-subrange scale, the Smagorinsky-Lilly constant (and constants appearing in the SGS TKE equation) can be theoretically determined, as demonstrated in Moeng and Wyngaard (1988).

Note that the SGS  $u_i'' \tilde{u}_j''$  term in (4) looks like the Reynolds stress term in the Reynolds average equations used in climate or mesoscale models, but it has a very different physical interpretation from the usual Reynolds stress term. The stress term appearing in (4) represents only the small turbulence, while the usual Reynolds stress represents *all* of the turbulent motion. The horizontal variations of the resolved motion in LES are as large as the vertical variations, and hence all derivatives in the SGS stress components,  $\partial u_i'' \tilde{u}_j'' / \partial x_j$  have to be included in (4), not just the  $\partial / \partial z$  component as in the Reynolds average equations.

The advection term in (4), i.e., the second term on the left-hand side, is highly nonlinear in nature. It includes not only the mean shear production for large turbulent eddies, but also the nonlinear vortex stretching and energy cascade effect which generates the small-scale turbulent motion. The numerical solution  $\tilde{u}_i$  of (4) is a detailed three-dimensional, time-evolving turbulent flow field for a given large-scale forcing.

Thus, LES is an excellent research tool for studying turbulent phenomena or acquiring turbulence statistics that depend mainly on large resolved eddies. For phenomena or statistics that depend largely on small-scale SGS eddies, such as chemical reaction or the near-surface statistics, LES should be used with great caution.

## 2.2 Weaknesses of LES

The LES technique requires a lot of computer resources. To properly resolve the three-dimensional large turbulent motions, a minimum resolution of  $\sim 40 \times 40 \times 40$  grid points is required. Our common practice today in simulating a convective PBL uses  $\sim 10^6$  grid points to cover a numerical domain of 3~5 km in the horizontal and 1~2 km in the vertical. Such a simulation thus resolves turbulent eddies down to  $\sim 50$  m in scale. A  $\sim 10^6$  grid LES, including the minimum five prognostic variables (the three wind components, buoyancy, and SGS energy) plus the pressure field, requires 15~20 Mws of computer memory and about 4 C90 seconds per time step. An LES time step is on the order of 1s, depending on the grid resolution and the maximum wind speed. Thus simulating a diurnal cycle with a  $96^3$  grid LES would take  $\sim 100$  C90 hours. And this covers only a few kilometers of the horizontal domain. Thus, LES cannot be possibly implemented into a large-scale meteorological forecast model in the foreseeable future. It will remain a stand-alone research tool for some time.

Besides being computationally expensive, LES has other weaknesses. The discrete representation of a continuous system invariably involves numerical approximations or truncation errors. The most notable error occurs in regions of strong mean gradient. The commonly-used centered-finite differencing schemes often give spurious overshoots in this region. Monotonic schemes have been used to eliminate this overshoot problem, but they are known to introduce large numerical diffusion, which may damp out desired turbulence motion or artificially enhance the entrainment rate. Another major uncertainty of LES comes from the treatment of the SGS turbulent motion; this problem is particularly serious near the surface (and perhaps in the entrainment zone) where eddies are small and unresolved. At the height below the horizontal grid mesh, i.e.,  $z < \Delta x$ , all eddies are unresolved and hence LES flow fields below this level are strongly dependent of the SGS model. For applications to stratocumulus-topped PBL, additional uncertainties arise from parameterizations of cloud microphysics and radiation.

Most of today's LESs are applied only to idealized, horizontally homogeneous PBLs mainly due to the size limitation of the numerical domain and the assumed periodic lateral boundary conditions. A typical LES domain is only several kilometers in the horizontal and hence cannot resolve any mesoscale variation. This limitation makes it difficult to simulate observational data, which often include some kind of mesoscale motions forced by surface or weather conditions. Mesoscale variations may drastically change the turbulence statistics, such as the horizontal velocity variances and hence the turbulent kinetic energy. Periodic lateral boundary conditions cannot be used for PBLs with inhomogeneous surface conditions, such as complex terrain. But applying an open inflow/outflow boundary condition poses a separate set of challenges.

### 2.3 Strengths of LES

Despite the above weaknesses, LES is still one of the best techniques we have today for studying turbulence. This is because LES can provide three-dimensional time-evolving turbulent flow fields, which can be used to examine the time evolution of coherent structures and their contribution to turbulent transport. The pressure field is difficult to measure in the field or in the laboratory. Traditionally, the pressure effect on the turbulent kinetic energy (TKE) budget could only be roughly estimated as the residual from the TKE budget obtained from field or laboratory measurements. LES allows us for the first time to directly calculate the pressure effect. LES can be used to perform “controlled” numerical experiments to isolate individual physical processes involved in the PBL. It can also be used to generate an extensive database of different PBL flow regimes to evaluate or develop PBL parameterization schemes. These strengths make LES a useful tool for investigating problems that are otherwise difficult to do through field measurements.

For these reasons, the number of LES users has been increasing drastically in recent years. We estimate just for PBL research, that about 20 LES codes have been developed independently worldwide during the past decade. And there are many more researchers who use an existing code developed by someone else. As an example, there are more than 30 research groups outside NCAR who use the NCAR LES for their research.

All LES codes are based on the same basic fluid equations: the Navier-Stokes equations. If the grid mesh is fine enough (so only the very small eddies need to be parameterized), LES solutions do not depend sensitively on the SGS modeling or numerics. This has been demonstrated in several intercomparison studies. The first PBL LES intercomparison took place in 1993 in which Nieuwstadt et al. (1993) compared the results of a free convective PBL simulation from four LES codes with differing SGS models and numerics. They found that, even with just a relatively coarse resolution (i.e.,  $40^3$  gridpoints), the agreement between these four models on turbulence statistics up to the third order moments is very good (e.g., Figure 1). They concluded that “in general model results lie within the scatter of available observations.” The second intercomparison study, summarized by Andr n et al. (1994), compared the same four LES codes but for a pure shear driven PBL. The results showed that using the same number of grid points (i.e.,  $40^3$ ), LES solutions are more sensitive to the SGS model (mainly in the lower one third of the PBL) for neutral than convective PBL simulation, but the overall agreement is still good.

Recently there were several more intercomparison studies of LES focusing on cloudy PBLs (Moeng et al., 1996; Bretherton et al., 1998), organized by the Boundary-Layer Cloud Working Group of GCSS (Global Energy and Water Experiment Cloud System Study). Those intercomparison studies gave encouraging results; different LES codes gave similar results on many turbulence statistics despite their differences in SGS turbulence or numerics.

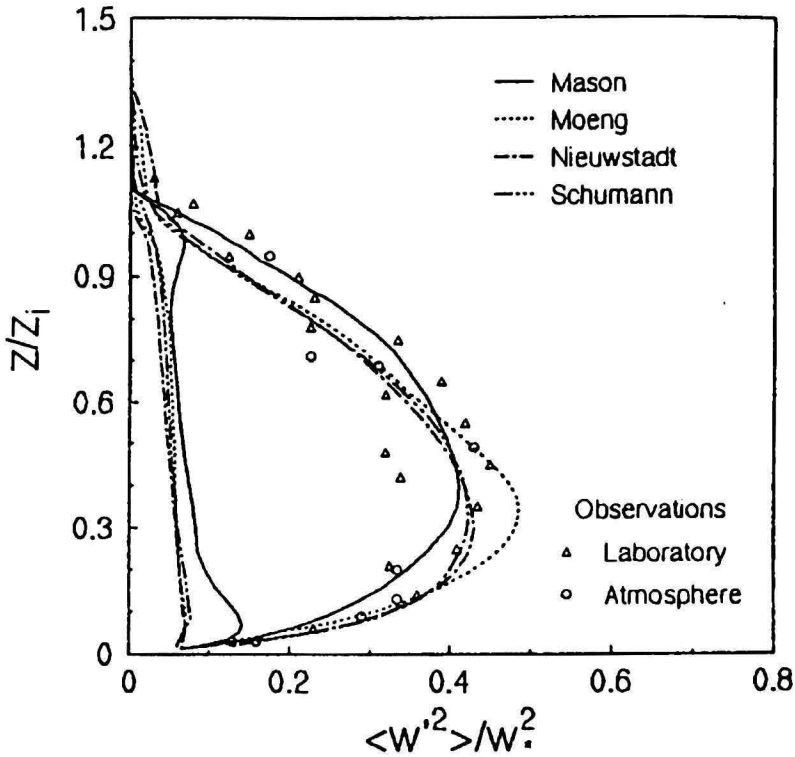


Fig. 1. The profiles of vertical-velocity variances from the four LES codes compared to observations (Nieuwstadt et al., 1993).

### 3 What Has LES Taught Us?

Since Deardorff's first calculation in 1970 (Deardorff, 1970a; Deardorff, 1972b) LES has made several scientific breakthroughs which have changed our views of PBL turbulence. Solutions from LES allowed us to visualize for the first time the 3D spatial and temporal evolution of turbulence in the PBL. An LES calculation by Schmidt and Schumann (1989) using  $160 \times 160 \times 48$  grid points revealed the eddy structure in great detail. Figure 2 shows a vertical cross section of an instantaneous flow field from a free convective PBL simulation ( $z_{i0}$  set to 1600 m, is the approximate PBL depth at the end of their simulation). It shows that updrafts (which are associated with warm thermals) are more intense and occupy a narrower area than downdrafts. These strong updrafts, with the size of the PBL depth, penetrate into the capping inversion, causing upward movement of the interface. On the sides of these penetrations, tongues of warm air occur and some of these tongues of warm air are eventually engulfed (or entrained) into the turbulent layer. This process results in

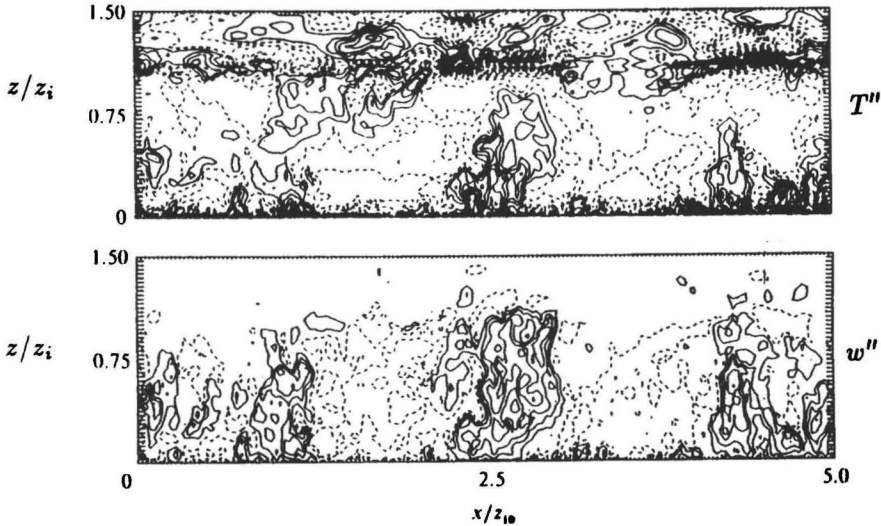


Fig. 2. Contour plots of temperature and vertical velocity fluctuations in a vertical cross section from an LES (Schmidt and Schumann, 1989).

the PBL growth.

In a plan view, both temperature and vertical velocity fields, shown in Figure 3, reveal spoke-like, irregular polygonal structure near the surface, which looks similar to that observed in the laboratory of Rayleigh-Benard convection. The intersections of these near-surface polygons are the likely locations where strong updrafts form. Higher up the PBL, thermals become more isolated. For shear-driven PBL, LES reveals a completely different coherent feature. There elongated high-low-speed streaks along the mean wind direction are simulated in the surface layer (Moeng and Sullivan, 1994; Lin et al., 1996), similar to those found in the wind tunnel or field measurements (Wilczak and Tillman, 1980).

LES also changes the way we scale the convective PBL statistics. Before Deardorff's 1972 LES calculations, turbulence statistics in both shear and convective PBLs were scaled with the friction velocity  $u_*$  and  $u_*/f$  where  $f$  is the Coriolis parameter. Based on his LES calculations, Deardorff found that better scales for the convective PBL are the convective velocity  $w_* \equiv [(g/T_0)z_i\overline{w\theta_0}]^{1/3}$  and the PBL depth  $z_i$ , rather than  $u_*$  and  $u_*/f$ . With these new scaling parameters, Lenschow et al. (1980) and many others, were able to nicely collapse measured or simulated data from different surface buoyancy forcings into universal curves. For example, the vertical velocity variance ( $\overline{w^2}$ ), the vertical flux of TKE ( $\overline{wE}$ ), and the dissipation rate ( $\epsilon$ ) measured from aircraft under different surface heating conditions scale well with  $w_*$  and  $z_i$ , as shown in Figure 4.

LES provided a revolutionary discovery about plume dispersion in the convective PBL. By releasing tracers at different heights in the 3D velocity

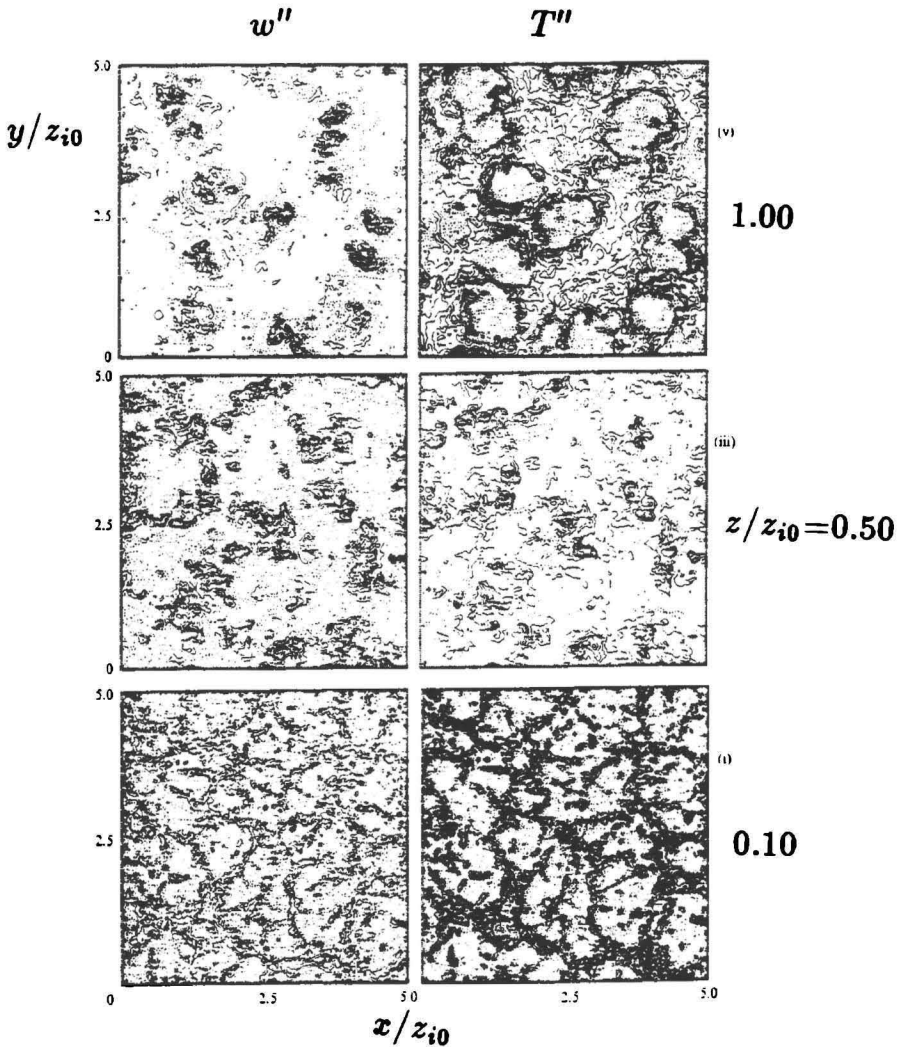


Fig. 3. Contour plots of temperature and vertical velocity fluctuations in horizontal cross sections from an LES (Schmidt and Schumann, 1989).

field from Deardorff's early LES, Lamb (1978) found that the maximum concentration of an elevated plume at first descends until it intercepts the ground, as shown in Figure 5. The descent of the elevated plume is due to the greater areal coverage of downdrafts. This finding, later confirmed by laboratory experiments (Willis and Deardorff, 1978) and field observations (Briggs, 1988), has an important application to air pollution; i.e., it shows the location and magnitude of the maximum surface concentration of source-released material. The above results provided the basis for the overhaul of short-range dispersion models in the 1980s (Venkatram and Wyngaard, 1988; Weil, 1994).

Another breakthrough from LES is the discovery of an asymmetric property of scalar turbulent diffusion. Conventional  $K$  models have, in an ad-hoc



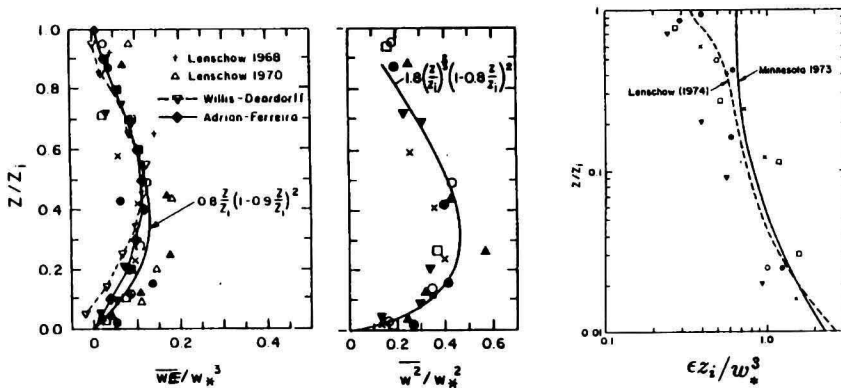


Fig. 4. Observed profiles of TKE flux, vertical-velocity variance, and TKE dissipation rate, all scaled with  $z_i$  and  $w_*$  (Lenschow et al., 1980).

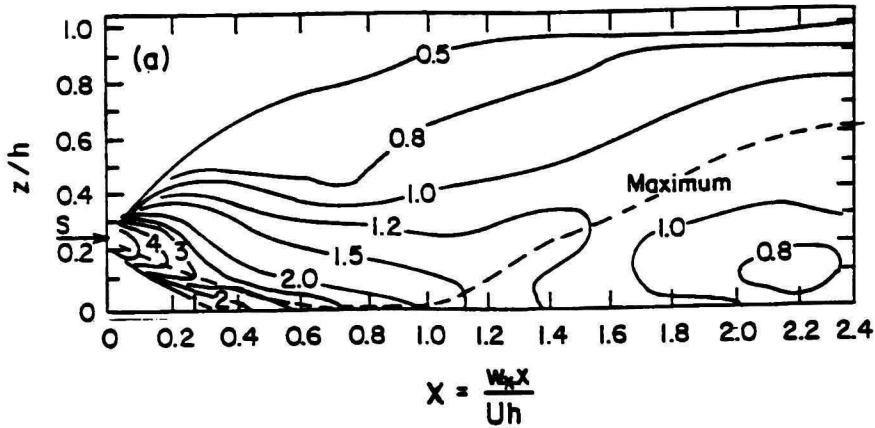


Fig. 5. The crosswind-integrated concentration fields in a convective PBL as predicted numerically from (Lamb, 1978).

way, used the same eddy diffusivity to describe the diffusion process of all scalars, including heat, moisture, and chemical species like ozone. Using LES, Wyngaard and Brost (1984) and Moeng and Wyngaard (1984) found that, in the convective PBL, a scalar that is released from the surface has a different eddy diffusivity than a scalar that is released from the PBL top. Wyngaard introduced two conceptual scalar fields: top-down  $c_t$  (which is ejected from the PBL top and has zero flux at the surface) and bottom-up  $c_b$  (which is ejected from the surface and has zero flux at the PBL top), and argued that any passive, conservative scalar can be linearly decomposed into these two components, i.e.,  $c = c_t + c_b$ . Under quasi-steady states, the fluxes of the top-down and bottom-up scalars are both linear in height, that is,  $\overline{w c_t} \sim \overline{w c_1} z/z_i$  and  $\overline{w c_b} \sim \overline{w c_0} (1 - z/z_i)$ , where  $\overline{w c_1}$  and  $\overline{w c_0}$  are the scalar fluxes at the PBL top and at the surface, respectively. Thus, the normalized top-down and bottom-up fluxes,  $\overline{w c_t}/\overline{w c_1}$  and  $\overline{w c_b}/\overline{w c_0}$  are symmetric about the mid-PBL.

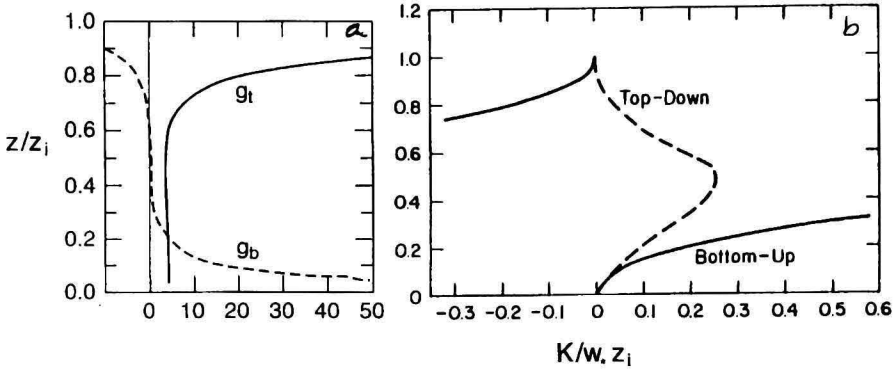


Fig. 6. a) The mean gradient functions and b) the resulting eddy diffusivities of the top-down and bottom up scalars from an LES.

LES showed that the mean gradient functions of the top-down and bottom-up concentrations,  $g_t$  and  $g_b$ , are *not* symmetric about the mid-PBL, as shown in Figure 6a (Moeng and Wyngaard, 1984), where

$$g_t \equiv -\frac{z_i w_*}{\overline{w c_1}} \frac{\partial C_t}{\partial z} \quad , \quad g_b \equiv -\frac{z_i w_*}{\overline{w c_0}} \frac{\partial C_b}{\partial z} . \quad (6)$$

Here  $C_t$  and  $C_b$  are the mean concentrations of the top-down and bottom-up scalar, respectively. While  $g_t$  remains positive throughout the whole PBL,  $g_b$  is positive in the lower half of PBL and becomes negative in the upper part. The negative gradient in  $g_b$  indicates the countergradient transport property—a bottom-up scalar can be transported by large thermals directly from the surface to the PBL top, without diffusing into the mid-PBL. The asymmetry feature of the gradient functions thus results in a different eddy diffusivity  $K$  ( $\equiv -\overline{w c} / (\partial C / \partial z)$ ) between the top-down and bottom-up scalars, as shown in Figure 6b (Wyngaard and Weil, 1991). While  $K$  of the top-down scalar remains positive in the whole PBL, the  $K$  value of the bottom-up scalar is ill-defined because of the countergradient property (see also discussion by Holtslag and Moeng, 1991). Furthermore, the  $K$  value of the bottom-up scalar is larger than that of the top-down scalar. This implies that the bottom-up scalar diffuses more effectively than the top-down scalar in the convective PBL.

Finally and most importantly, LES has brought into PBL research a quantitative and detailed measure of the turbulence statistics. With LES we are able to document the statistical distributions throughout the PBL, and then use them to study long-standing closure problems in PBL modeling, as discussed in section 4.5.

## 4 Recent Progress in PBL LES Research

### 4.1 Improvements in SGS modeling

The SGS effect is largest near the surface where the energy-containing eddies are small. Hence, the major uncertainty of LES lies in this near-wall region. A critical review of the near-wall SGS problems and methods to improve the SGS modeling in LES can be found in Mason (1994). Here, only a couple of SGS modeling studies that aimed at improving the surface layer prediction will be mentioned.

It is known that the traditional Smagorinsky-Lilly SGS model produces mean wind and temperature profiles in the surface layer that deviate from Monin-Obukhov (M-O) similarity (i.e., the law-of-the-wall theory). Mason and Thomson (1992) showed that by introducing stochastic backscatter in their Smagorinsky SGS model, much better agreement between LES and M-O similarity forms can be obtained. Alternatively, Sullivan et al. (1994) developed a two-part eddy viscosity model, which in addition to the fluctuating Smagorinsky-type eddy viscosity includes a mean-field eddy viscosity. The mean-field eddy viscosity is devised to recover the similarity behavior in the absence of any resolved turbulence. Their two-part eddy viscosity model produces mean wind and temperature profiles that agree well with the M-O prediction in the surface layer and hence gives a significant improvement over profiles produced using the standard Smagorinsky-type model.

### 4.2 Implementation of nested-grid LES

LES solutions become less sensitive to the SGS modeling when the grid mesh is finer. Therefore, another way to enhance the accuracy of LES is by increasing the grid resolution. Today's LES are often performed with  $\sim 10^6$  grid points, which is almost an order magnitude larger than Deardorff's first LES.

Because eddies in mid-PBL are relatively larger than those near the surface and thus easier to resolve with a typical LES grid, an effective way of enhancing resolution is to adopt fine grid only at regions where energy-containing eddies are smaller, such as near the surface. For that purpose, Sullivan et al. (1996) developed a two-way interacting grid nesting LES where the horizontal extent of the nested grid is the same as that of the outer grid but its vertical domain can be much smaller than the outer grid. This fine-grid layer can be positioned anywhere within the vertical domain of the PBL where fine resolution is desired. In their first nesting-grid experiment, Sullivan et al. applied the fine-mesh layer in the surface layer for a weak convection, strong shear PBL, and were able to obtain detailed eddy structure near the surface.

From this study, Sullivan et al. found that increased resolution in the surface layer does not appreciably alter the ensemble-mean statistics of the resolved and SGS motions above the surface layer. This implies that the turbulence structure within the bulk of the PBL is not sensitive to the near-surface turbulence, even though the shear and buoyancy instabilities originate at the surface. This supports the basis of LES; LES cannot possibly resolve small eddies very close to the surface but it is still able to provide reasonable structure in the bulk of the PBL. Khanna and Brasseur (1997) applied a similar nesting to the surface layer to study the effect of  $z_i$  scaling on the turbulent structure in the surface layer.

By applying a nested grid with fine resolution to the entrainment zone, Sullivan et al. (1998) and Moeng et al. (1998) were able to simulate the entrainment processes (and hence deduce the entrainment rate) for surface-heating and cloud-top-radiative-cooling driven PBLs. As an illustration, Figure 7 taken from Sullivan et al. (1998) shows the spatial and temporal interaction of an active thermal plume with the overlying stable inversion for a clear surface-heating driven PBL, and the resulting entrainment. These entrainment events are well resolved by the LES; the mesh spacing in the entrainment zone is depicted in the upper right corner of each panel. In panels a) - d), we see a vigorous updraft (located at  $Y \sim 2000$  m) impinging onto the capping inversion; the updraft pushes the inversion upward and increases the local stratification just above it. The rotational motions which form inside the thermal plume are sufficiently strong to fold over the interface and draw in inversion air, resulting in entrainment at the edge of the plume. At later times, panels e) - h), the distorted interface leads to the formation of a pocket of warm air that extends below the nominal inversion height. This pocket of warm air is pulled down and pinched off by the strong return flow of the plume, thus leading to entrainment. These engulfing and pinching-off mechanisms, well resolved in the current LES, are seen to be responsible for most of entrainment in the simulated buoyancy-driven PBL.

### *4.3 Inclusion of radiation and microphysics for cloudy PBLs*

To apply LES to a cloudy PBL, many more physical processes have to be incorporated into LES codes. Because longwave radiative cooling at the cloud top provides one of the major buoyancy forces that drive turbulence within stratocumulus-topped PBLs, a longwave radiation scheme is needed to simulate such a PBL. For our purpose, we use very simple longwave radiation schemes; cloud drops are assumed to act like a greybody absorber, which facilitates simplified approaches to the radiative transfer calculations. Admittedly, such are simplified compared to the treatment of turbulent motion in LES. The idea is to treat the calculated longwave radiative cooling field as a forcing for driving turbulence. Any quantitative uncertainty in calculating such a

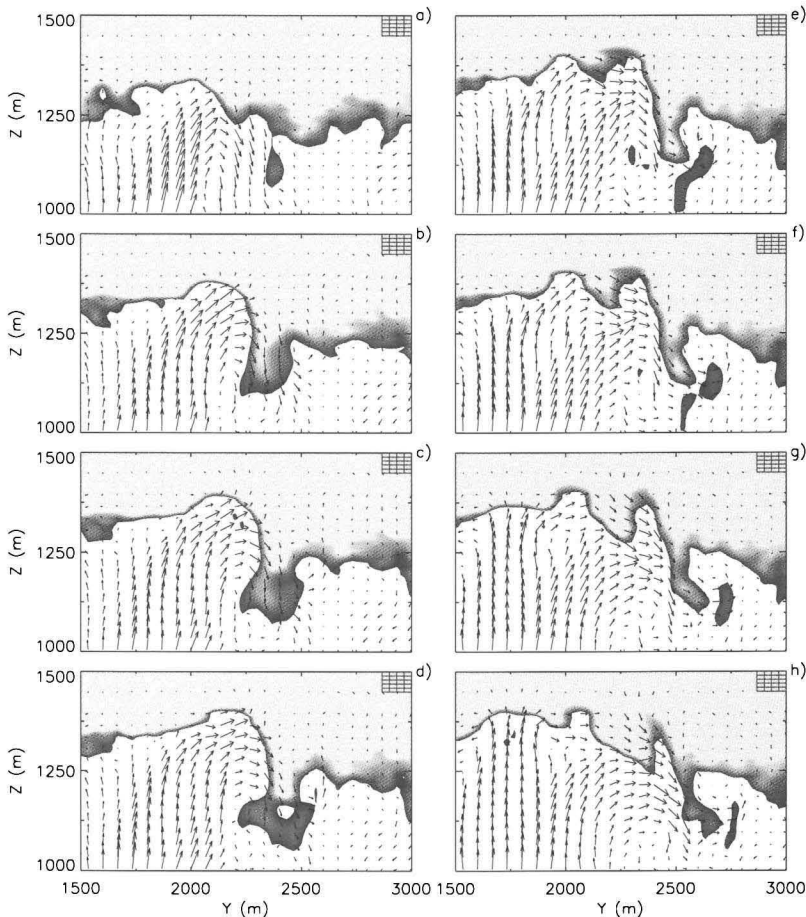


Fig. 7. Temporal and spatial evolution of flow (shown by arrows) and temperature (shown by grey-color contours) fields near the inversion in a limited LES domain (Sullivan et al., 1998) .

radiative forcing may affect the absolute value of the simulated turbulent intensity and fluxes, such as buoyancy flux and TKE. But, with proper scaling, such as the velocity scale  $w_{*c} \equiv (2.5(g/T_0)z_i B)^{1/3}$  (where  $B \equiv \int_0^{z_i} \overline{w\theta_v} dz/z_i$  is the layer-averaged buoyancy flux) proposed by Deardorff (1980), turbulent statistics (magnitude and vertical distribution) in the cloud-top-radiatively-driven PBL may be universally described regardless of the actual amount of the radiative forcing.

Today very few LESs include solar radiation for studying cloud albedo or diurnal cycle of marine stratocumulus regime. This is perhaps due to the

difficulty (and extra computational expense) in incorporating a solar radiation scheme into LES. Dudda et al. (1996) used a 3D cloud field simulated from an LES to study the effects of horizontal inhomogeneity of a cloud field on cloud albedo calculation. They found that the cloud albedo computed from a 1D radiative transfer model agreed well with that from a 2D method.

The effects of cloud microphysics include latent heating and drizzle formation. For LES studies that are focused only on latent heating effects, simple bulk microphysics schemes are often used. For those interested in drizzle formation (Stevens et al., 1998) or droplet size distributions (Kogan et al., 1995; Stevens et al., 1996), detailed cloud microphysics models, which solve for a spectrum of droplets with different sizes (called bin models or explicit schemes) are often adopted. As mentioned above, LES is not a proper tool to investigate physical processes that depend on small-scale turbulent motions. It remains unclear whether the cloud microphysics depends strongly on the small-scale motion, but so far the above LES studies were able to obtain useful information on the effects of cloud microphysics on PBL turbulent structure. However, simulated quantities (such as liquid water content or cloud fraction) that may depend strongly on the cloud microphysical treatment should be interpreted carefully.

#### *4.4 Application to different PBL flow regimes*

Within the past several years, LES has been applied not only to the clear-air atmospheric PBL but also to oceanic PBLs, canopy turbulence, cloud-topped PBLs and many other applications. For instance, it has been applied to study the oceanic mixed layer since 1993 (McWilliams et al., 1993; Wang et al., 1996). Adding the Stokes drift effect into the LES equation, Skillingstad and Denbo (1995) and McWilliams et al. (1997) were able to simulate Langmuir turbulence and examine the structure of Langmuir circulations and their effect on turbulence intensity and transport. LES has also been applied to investigate turbulence within a canopy (Shaw and Schumann, 1992; Kanda and Hino, 1994). These studies showed promising results: Not only the vertical distributions of turbulent statistics, such as Reynolds stress and turbulence intensity, but also large-eddy structures, such as sweep and ejection events, from such simulations compare well with observations. LES has also made an impact on diffusion studies. Weil et al. (1997) extended Lamb's LES work to investigate the diffusion properties in other PBL regimes; Schumann (1989) used LES to explore chemically reacting scalars; and Henn and Sykes (1992) used LES to examine the concentration fluctuating field downstream of elevated sources.

One of the most intensive applications of LES in recent years has been to the marine stratocumulus regime, which plays a major role in cloud and climate. The LES technique has been applied to study cloud-top entrainment instability (Deardorff, 1980a; Moeng et al., 1995); to isolate effects of radiative

cooling, entrainment, and surface heating processes (Moeng et al., 1992); to simulate detailed microphysical interactions (Kogan et al., 1995; Stevens et al., 1996); to examine the effect of drizzle on turbulence structure and transport (Stevens et al., 1998); and to investigate entrainment of radiatively-driven PBL (Bretherton et al., 1998; Moeng et al., 1998a). More than ten LES research groups worldwide have joined the GCSS Boundary-Layer Cloud Working Group (Moeng et al., 1996; Bretherton et al., 1998) in studying cloudy PBL regimes.

LES has also been applied to study Arctic leads (Glendening and Burk, 1992), cloud development during cold air outbreaks (Chlond, 1992); trade-wind cumulus (Siebesma and Cuijpers, 1995); boundary-layer clouds with ice (Rao and Agee, 1996), stable PBLs (Mason and Derbyshire, 1990; Kosovic and Curry, 1997), and baroclinic PBLs (Brown, 1996) to name a few.

#### 4.5 Development of PBL parameterizations

There exist many PBL parameterization schemes (i.e., ensemble-mean closure models); e.g., the second-order closure technique, bulk modeling, eddy diffusivity modeling, transilience theory, mass flux approach, and K-profile approach (see chapter 1 and 4). They were developed to model the *net* effect (i.e., ensemble-mean statistics) of all turbulent motions within the PBL in large-scale meteorological forecast models. We pointed out in section 1 that several LES intercomparison studies have shown that many turbulence statistics do not depend sensitively on the parameterization of SGS physics and numerics in LES. For that reason, LES can be used as a database for developing/evaluating the above PBL parameterization schemes. Since Holtslag's and Duynkerke's chapters also cover the PBL (ensemble-mean) modeling topic, only a brief review on the use of LES in developing PBL parameterizations will be given here.

There are two ways LES can be used in developing or calibrating PBL parameterizations. One is to use LES solutions as the standard of comparison to evaluate the system performance of PBL parameterizations. By system performance, we mean the accuracy of the prediction of PBL outputs, such as the PBL mean and flux fields of momentum, temperature or other scalars that are of importance to forecast models. One such study was carried out by Ayotte et al. (1996). They generated ten PBL flow regimes, ranging from neutral to strongly convective, and with a weak to strong capping inversion. They then compared the outputs from six generic PBL models (most of which are currently used in general circulation models) with the LES solutions. One of their findings is that all of these models have difficulty in reproducing the entrainment at the top of PBL in most PBL regimes. They also explored the sensitivity of PBL model results to vertical resolution in the PBL and showed that most of the PBL models performed poorly with the coarse resolutions

commonly used in general circulation models.

Another way of using LES in developing/calibrating PBL parameterizations is to check the appropriateness of individual closure assumptions. Every PBL parameterization scheme requires closure(s). For example, to close the system of governing equations in a second-order closure model, assumptions are needed for all the pressure-related quantities. The NCAR LES model, has been used extensively in studying closures: in examining the pressure-related, turbulent-transport and dissipation-rate terms in the second-order closure model equations (Moeng and Wyngaard, 1986; Moeng and Wyngaard, 1989; Andren and Moeng, 1993); in developing a transport matrix for an integral closure model (which is similar to Stull's transilience scheme) (Fiedler and Moeng, 1985); in developing new bulk models (Randall et al., 1992; Otte and Wyngaard, 1996); in quantifying the mass flux and updraft/downdraft properties which are needed in closing the mass flux modeling approach (Schumann and Moeng: 1991a; Schumann and Moeng: 1991b; Wyngaard and Moeng, 1992; Moeng et al., 1992) in improving the representations of eddy diffusivity and countergradient transport for K-profile models (Holtslag and Moeng, 1991; Large, et al., 1994). The research group at KNMI and IMAU has also used their LES intensively to evaluate the mass flux closure schemes for shallow cumulus convection (Siebesma and Cuijpers, 1995).

## 5 Concluding Remarks

In this chapter, we reviewed several LES studies that have advanced our understanding of PBL turbulence and mixing properties. We also reviewed recent progress on PBL LES research, in the areas of code development and applications to more complicated PBL regimes, such as cloudy PBLs, PBLs with stable stratification, and turbulence within a canopy and ocean mixed layer. The major use of LES so far included (1) better understanding turbulent coherent structures, (2) examining physical processes involved in the PBL, particularly in cloudy PBLs, and (3) generating databases in developing/evaluating PBL parameterizations for use in large-scale meteorological forecast models.

The major uncertainty of LES lies in the SGS modeling, especially in the near surface region. The SGS problem is greatly amplified when LES is applied to the very stable PBL; stable stratification can suppress turbulent mixing and therefore the specification of the SGS length scale becomes problematic. Similar problems occur in the entrainment zone where turbulence advances into a stably stratified layer. However, improvements to the SGS modeling for LES have been rather limited, mainly because of the lack of an experimental or observational basis for making such an improvement. Recently, field campaigns to provide detailed information on the small-scale (SGS) turbulent motion have been proposed (Tong et al., 1998), which should provide useful data in



improving and designing the SGS modeling for LES.

In order to apply LES to more complicated, more realistic PBL flow regimes, we are now facing many challenges. For example:

- Understanding and overcoming the uncertainties in simulations of PBLs with stratocumulus or trade-wind cumulus. Recent LES intercomparison studies have shown that many climate-important PBL parameters, such as the entrainment rate, cloud fraction, and liquid water path, are sensitive to the treatment of numerics, SGS turbulence, radiation, and SGS microphysical processes. To use LES as a database for developing PBL cloud schemes, these uncertainties have to be addressed first. How to accurately represent parameterized physical processes (such as longwave radiation and cloud microphysics) in LES remains a challenge.
- Simulating the very stable PBL where the negative buoyancy effect is comparable to the shear production in the TKE budget and where gravity waves significantly affect the turbulent motion. Turbulence in this case is spatially and temporally intermittent, and is very poorly understood. This PBL also depends sensitively on the underlying surface condition, such as terrain slope.
- Studying the effect of ocean surface waves on the surface fluxes. This effect may have a large impact on air-sea interaction. The main challenge for LES is in implementing a surface-wave-following coordinate so some surface wave effects can be resolved explicitly.
- Simulating PBLs over non-periodic complex terrain. This problem is similar to that of studying ocean surface wave effect. It requires a terrain-following coordinate. Additional difficulty in this problem is the description of turbulent inflows at the lateral boundary. How to input a chaotic flow field at the inflow boundary remains a problem.

## **Acknowledgment**

I thank Bjorn Stevens, Peter Sullivan, and Jeff Weil for reading the manuscript and providing useful inputs.

